Experiment

1.1 Materials

Melamine, Potassium Bromide, Ammonia, Ethanol. All of these were directly used without any further treatment.

1.2 Characterization

The structures of catalysts were characterized and revealed by X-ray diffraction (XRD, Bruker D8 Advance), Fourier transform infrared spectroscopy (FTIR, Nicolet IS50), X-ray photoelectron spectroscopy (XPS, Thermo Scientific K-Alpha). Ultraviolet-visible spectrophotometry (UV-vis, Lambda 650S) was utilized to reveal the optical property. Scanning Electron Microscopy (SEM, WU8010 FE-SEM) and Transmission Electron Microscopy (TEM, JEOL JEM-F200) were used to analyze the morphology, while the specific surface area was conducted by Nitrogen Adsorption-Desorption BET Surface Area Analyzer (Micromeritics ASAP 2460). Photoluminescence spectroscopy (PL, Edinburgh FLS1000) was employed to investigate the dynamics of charge carriers.

2.1 Catalyst synthesis

2.1.1 Preparation of PCN

5 g melamine were calcined at 550 °C for 240 min with a heating rate of 10 °C/min.

2.1.2 Preparation of NCN

1 g PCN was placed in a tube furnace and heated to 500 °C at a heating rate of 10 °C/min under an ammonia vapor. After kept in this temperature for 1 hour, NCN was obtained after cooled down to the room temperature.

2.1.3 Preparation of KCN

0.4 g NCN and 3 g KBr were mixed and grounded together for 10 minutes. Under a nitrogen atmosphere, the mixture was heated to 500 °C at a heating rate of 10 °C/min and maintained at this temperature for 2 hours. After cooled down to the room temperature, the yellow powders were washed with deionized water. KCN was obtained by drying the wet powders.

2.1.4 Preparation of PCNK

PCNK was directly synthesized by mixing PCN (0.4 g) and KBr (3 g). And then, the

mixtures were heated under 500 °C for 2 h. After cooled down to the room temperature, the powders were washed with deionized water. PCNK was obtained by drying wet powders.

2.2 Photocatalytic $H_2O_2$ production

20 mg KCN and deionized water (27 mL) and ethanol (3 mL) were added into the independent quartz tubes. The pure $O_2$ bubbled into the reactor. Then, the reactor was placed in liquid $N_2$ to coagulate. After multiple rounds of gas replacement, the reactor was full of $O_2$ to balance. The reaction was conducted at 25 °C under 300 W Xenon lamp ($\lambda \geq 420$ nm) for 1 h. After reaction, the concentration of $H_2O_2$ was monitored by measuring absorbance of $Ti^{IV}$- $H_2O_2$ yellow complex with UV-Vis spectra at 410 nm.

Figure S1. SEM images of PCN (a) and NCN (b).

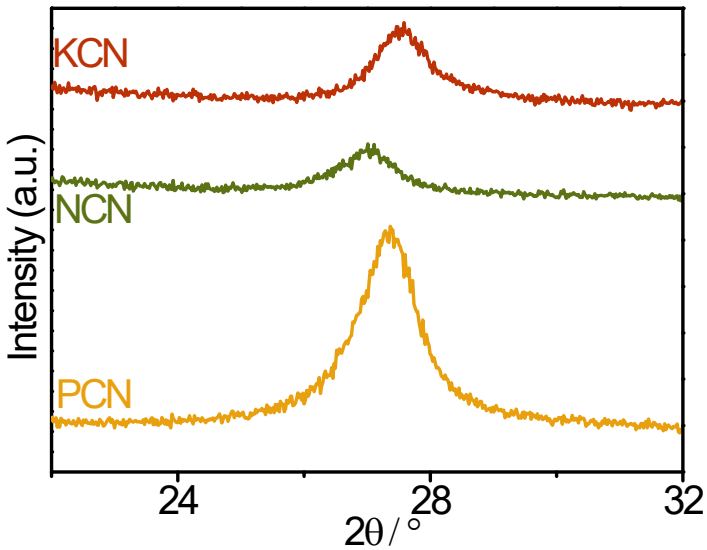


Figure S2. Enlarged XRD patterns.

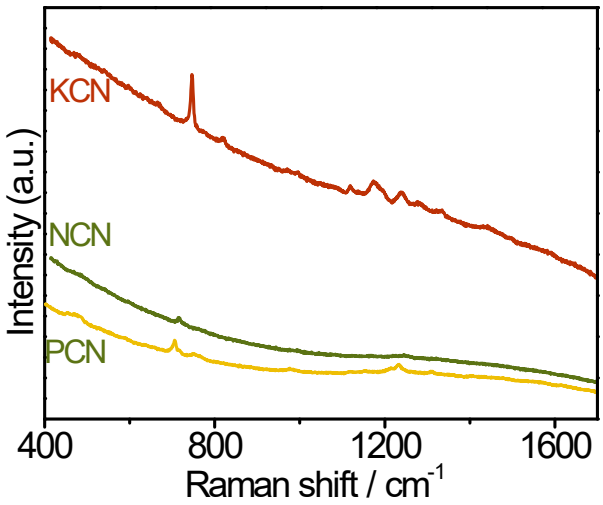


Figure S3. Raman spectra of samples.

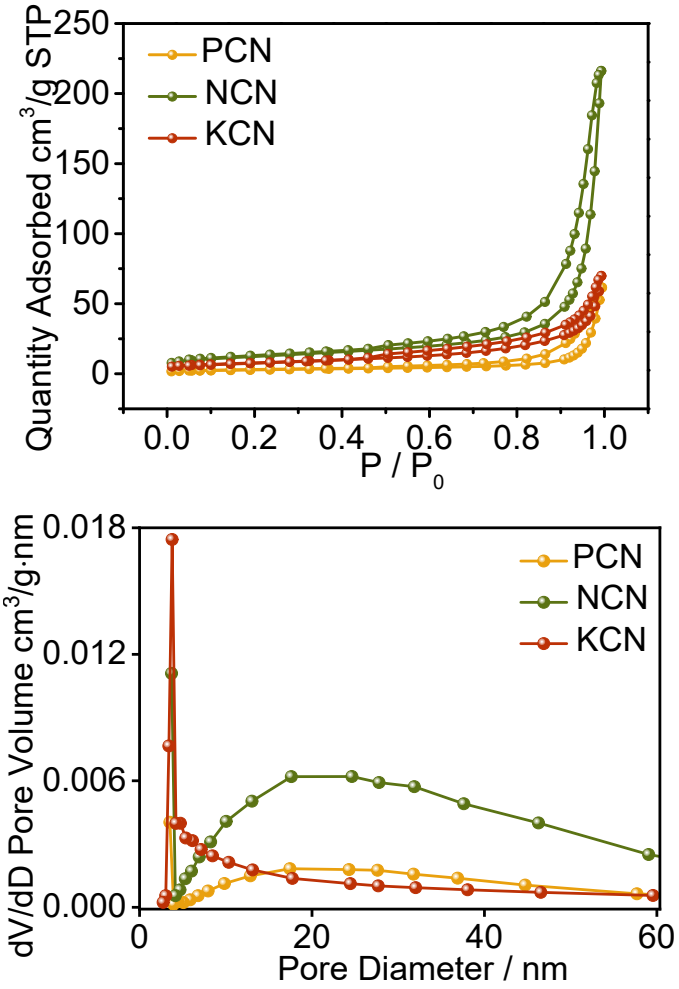


Figure S4. BET surface areas and average pore diameters of samples.

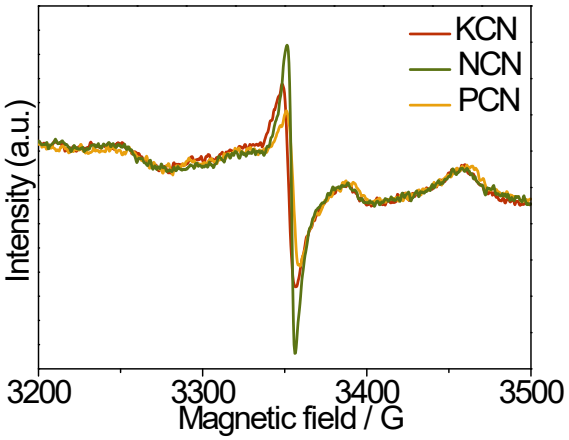


Figure S5. The EPR spectra of samples

Table S1. The carbon and nitrogen contents of PCN, NCN and KCN in XPS and elemental analysis.

| Sample | PCN | NCN | KCN |
|---|---|---|---|
| Carbon (wt.%) | 46.25 | 45.07 | 43.96 |
| Nitrogen (wt.%) | 50.03 | 51.83 | 44.47 |
| Carbon (%) (EA) | 34.9 | 34.5 | 27.0 |
| Nitrogen (%) (EA) | 63.3 | 63.6 | 50.1 |

Table S2. The binding energy and areas of XPS C 1s in PCN, NCN and KCN.

| Sample | C-C/C-H | | | C≡N | | | N-C=N | | |
|---|---|---|---|---|---|---|---|---|---|
| | Binding Energy | Area | % | Binding Energy | Area | % | Binding Energy | Area | % |
| PCN | 284.9 | 22327 | 29.4 | - | - | - | 288.4 | 53561 | 70.6 |
| NCN | 284.7 | 20539 | 25.5 | - | - | - | 288.1 | 60001 | 74.5 |
| KCN | 284.7 | 24336 | 30.1 | 286.9 | 10932 | 13.5 | 288.1 | 45607 | 56.4 |

Table S3. The binding energy and areas of XPS N 1s in PCN, NCN and KCN.

| Sample | C-N=C | | | $(C)_3$-N | | | C-$NH_x$ | | |
|---|---|---|---|---|---|---|---|---|---|
| | Binding Energy | Area | % | Binding Energy | Area | % | Binding Energy | Area | % |
| PCN | 398.6 | 61192 | 50.7 | 399.3 | 49351 | 40.9 | 401.0 | 10115 | 8.4 |
| NCN | 398.6 | 86350 | 64.4 | 399.5 | 38808 | 29.0 | 401.0 | 8859 | 6.6 |
| KCN | 398.5 | 71291 | 62.8 | 399.1 | 29970 | 26.4 | 400.9 | 12219 | 10.8 |

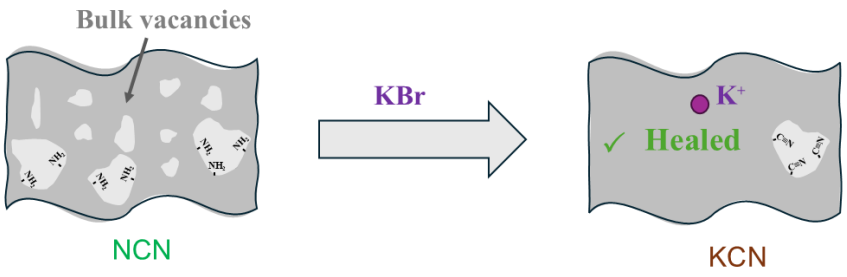


Figure S6. The schematic diagram of KCN formation.

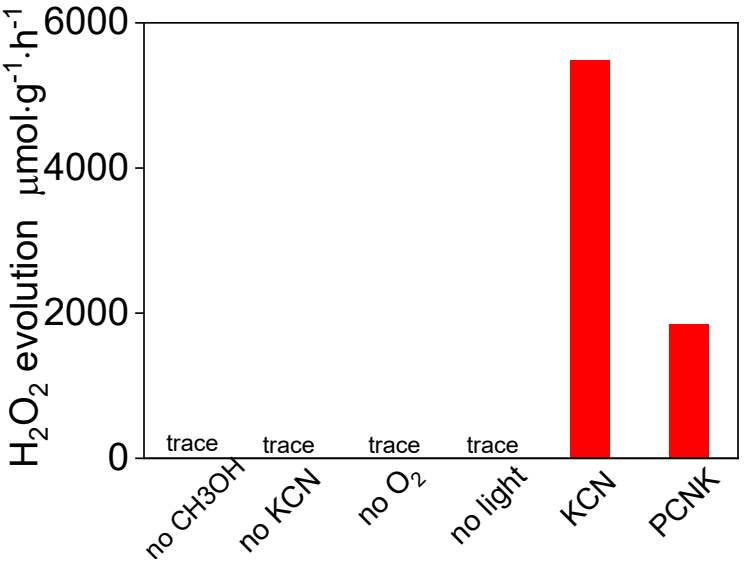


Figure S7. Bulk experiments of photocatalytic $H_2O_2$ evolution.

Table S4. Compared photocatalytic $H_2O_2$ production performances with different carbon nitride catalysts.

| Catalyst | $H_2O_2$ evolution rate / μmol·g$^{-1}$·h$^{-1}$ | AQY / % | Sacrificial agent | Ref. |
|---|---|---|---|---|
| 10% ZnO/g-$C_3N_4$ | 1112.43 | - | Ethanol | 27 |
| Au/g-$C_3N_4$ | 1052 | - | IPA | 28 |
| Cu-NG/CN | 2856 | - | Ethanol | 29 |
| $R_{370}$-CN | 170 | ~4.3 | - | 30 |
| SeCN | 903.01 | - | IPA | 31 |
| MCN | 1147.03 | - | IPA | 32 |
| TCN-520 | 93.89 | - | Ethanol | 33 |

| | | | | |
|---|---|---|---|---|
| KCN | 5488 | 7.4 | Ethanol | This work |


Figure S8. The pH value of solvent before and after $H_2O_2$ photosynthesis.

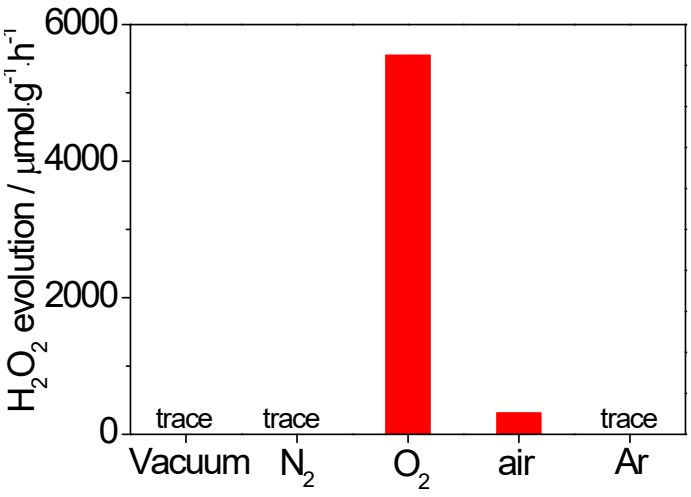


Figure. S9. $H_2O_2$ photosynthesis performance of KCN under different gas atmosphere.

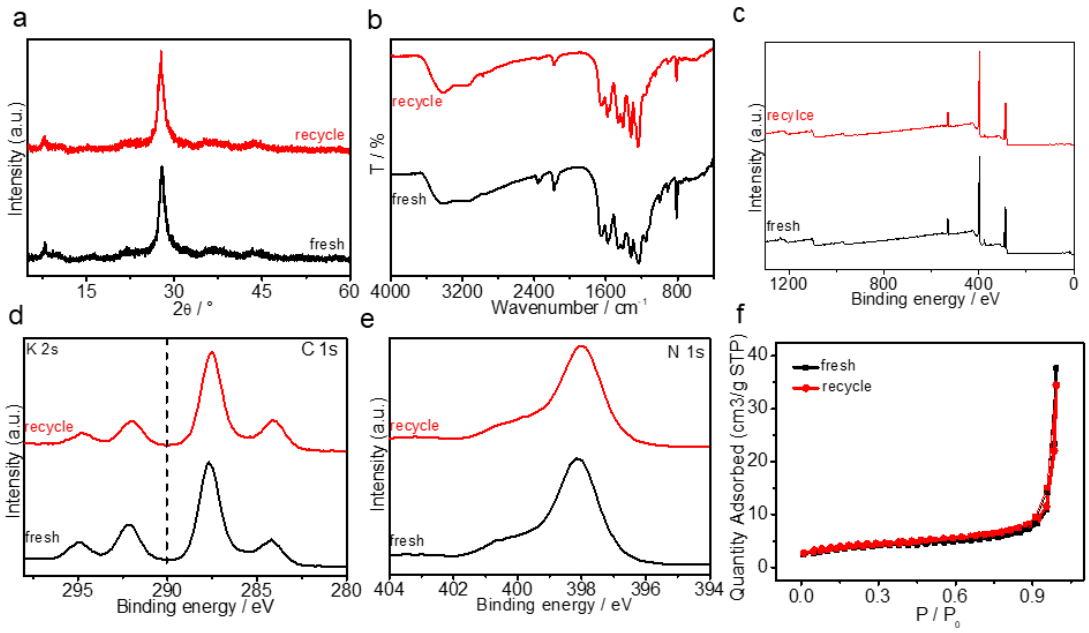


Figure S10. (a) The XRD pattern, (b) FT-IR spectra, (c) XPS survey spectra, (d) high resolution XPS C 1s and K 2s spectra, (e) high resolution XPS N1 spectra, (f) BET spectra

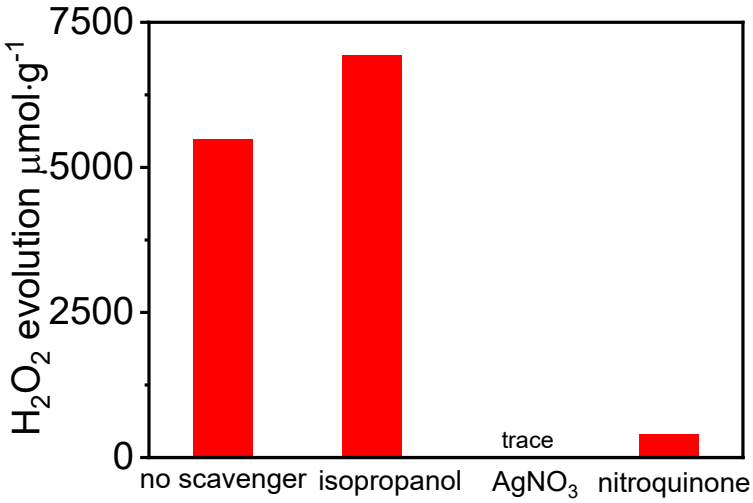

Figure S11. $H_2O_2$ photosynthesis performances under various scavengers.

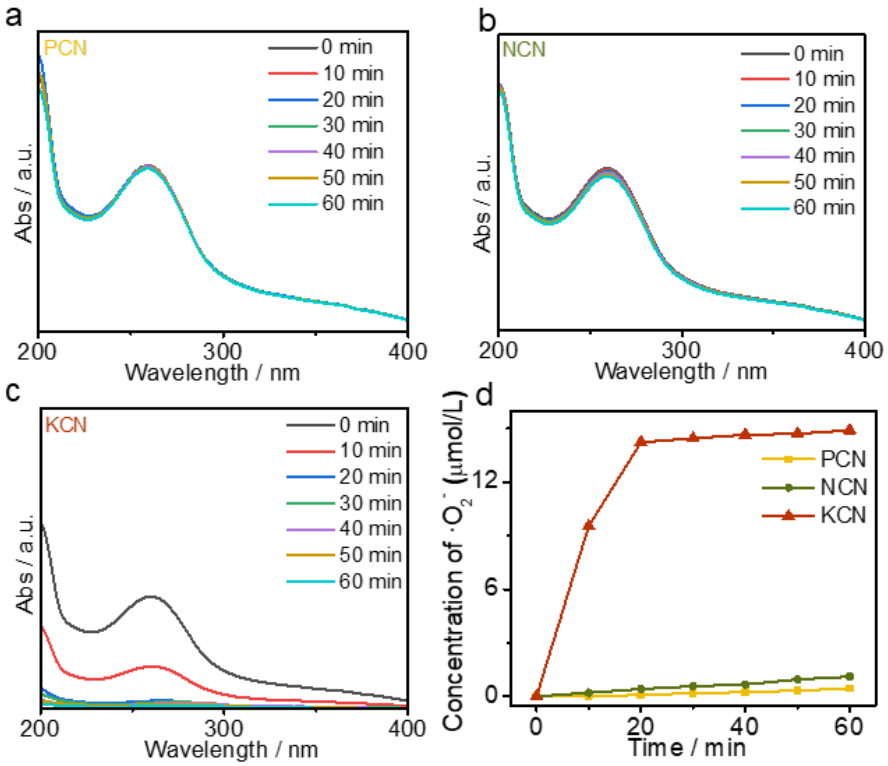


Figure S12 (a-c) UV-Vis spectra of NBT degradation over PCN, NCN and KCN, (d) Time dependent degradation of NBT to detect $\cdot O_2^-$.

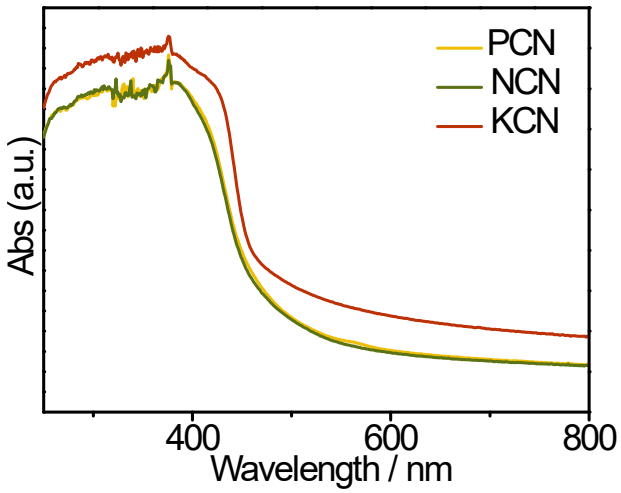

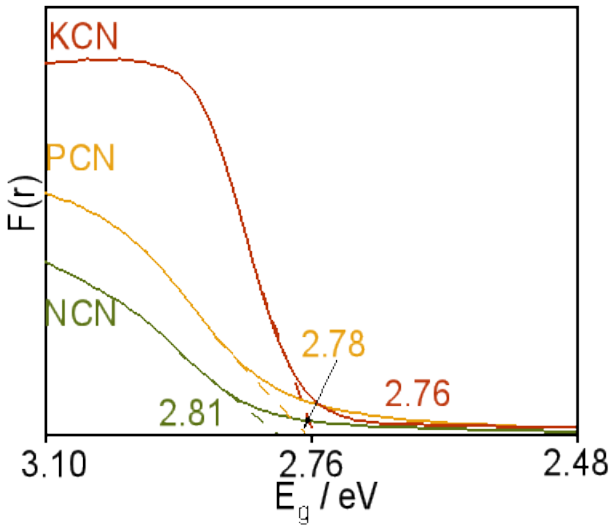


Figure S13. The UV-Vis spectra and Band gaps of samples

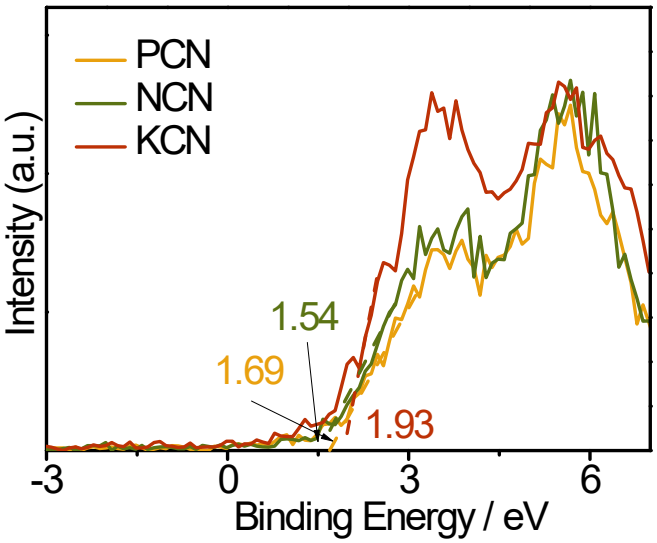


Figure S14. XPS valence band spectra.

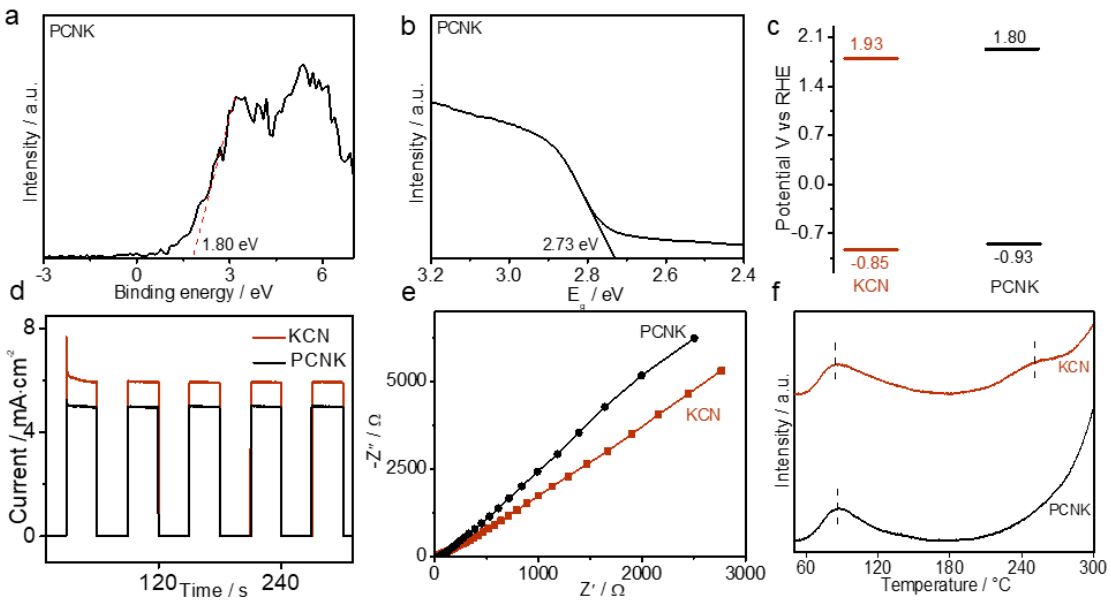


Figure S15. (a) XPS valance spectra and (b) DRS spectra of PCNK, (c) band structure and PCNK and KCN, (d) transient photocurrent spectra, (e) EIS spectra and (f) $O_2$-TPD spectra of PCNK and KCN.

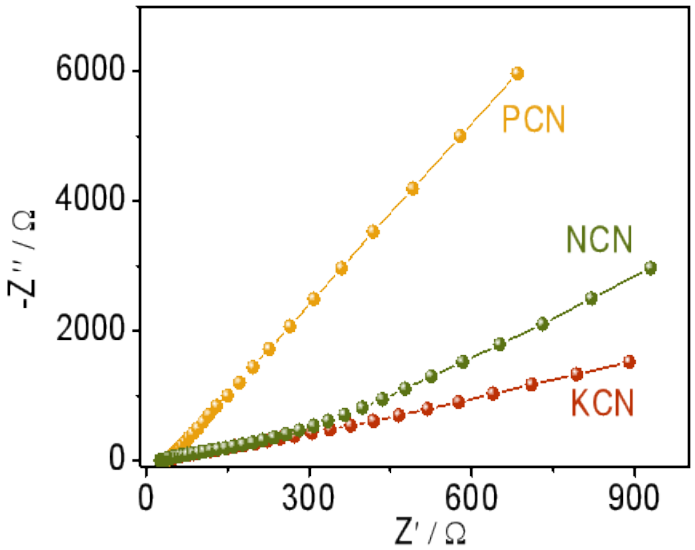


Figure S16. EIS spectra

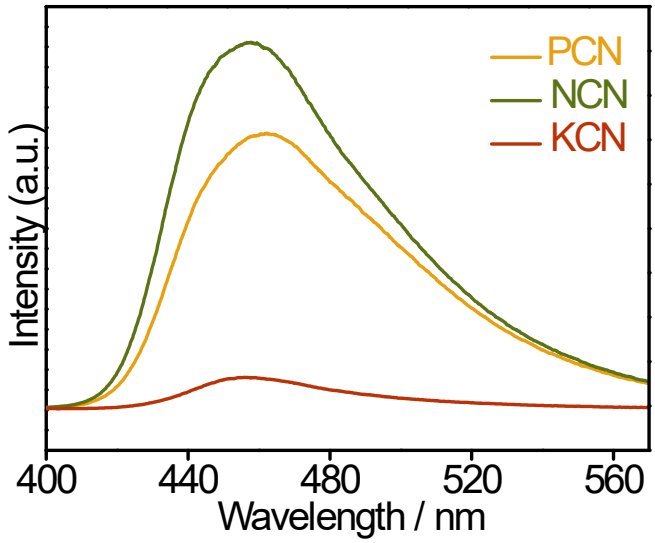


Figure S17. Steady PL spectra.

Table S5. The decay components of the PL lifetimes of different samples.

| Sample | $\tau_1$ / ns | % | $\tau_2$ / ns | % | $\tau_3$ / ns | % |
|---|---|---|---|---|---|---|
| PCN | 1.51 | 35.88 | 5.91 | 48.87 | 31.39 | 15.25 |
| NCN | 1.50 | 28.81 | 5.67 | 52.87 | 28.61 | 18.32 |
| KCN | 0.31 | 59.93 | 2.59 | 40.07 | - | - |